© 2016. Published by The Company of Biologists Ltd | Journal of Cell Science (2016) 129, 3781-3791 doi:10.1242/jcs.196196

RESEARCH ARTICLE

Atg9A trafficking through the recycling endosomes is required for autophagosome formation

Kenta Imai[1], Feike Hao[2,3], Naonobu Fujita[1,4], Yasuhiro Tsuji[1], Yukako Oe[1], Yasuhiro Araki[3], Maho Hamasaki[1,2], Takeshi Noda[1,3,*] and Tamotsu Yoshimori[1,2,*]

ABSTRACT

Autophagy is an intracellular degradation pathway conserved in eukaryotes. Among core autophagy-related (Atg) proteins, mammalian Atg9A is the sole multi-spanning transmembrane protein, and both of its N- and C-terminal domains are exposed to the cytoplasm. It is known that Atg9A travels through the trans-Golgi network (TGN) and the endosomal system under nutrient-rich conditions, and transiently localizes to the autophagosome upon autophagy induction. However, the significance of Atg9A trafficking for autophagosome formation remains elusive. Here, we identified sorting motifs in the N-terminal cytosolic stretch of Atg9A that interact with the adaptor protein AP-2. Atg9A with mutations in the sorting motifs could not execute autophagy and was abnormally accumulated at the recycling endosomes. The combination of defects in autophagy and Atg9A accumulation in the recycling endosomes was also found upon the knockdown of TRAPPC8, a specific subunit of the TRAPPIII complex. These results show directly that the trafficking of Atg9A through the recycling endosomes is an essential step for autophagosome formation.

KEY WORDS: Autophagy, Atg9, Sorting motif, Golgi, Recycling endosome, TRAPP, AP-2

INTRODUCTION

Macroautophagy, hereafter called autophagy, is a process induced by starvation during which intracellular material is degraded and recycled for cellular homeostasis. In addition to such a function, autophagy plays numerous important physiological roles, such as in damaged organelle clearance, providing cellular immunity against invading pathogens, and tumor suppression (Kawabata and Yoshimori, 2016). In the process of autophagy, a double-membrane structure, called an autophagosome, is formed to sequester and deliver cytosolic proteins and organelles into the lysosomes. The formation of an autophagosome depends on a series of autophagy-related (Atg) proteins that are highly conserved from yeast to mammals and are required for autophagosome formation (Nakatogawa et al., 2009; Shibutani and Yoshimori, 2014).

[1]Graduate School of Frontier Bioscience, Osaka University, 2-2 Yamadaoka, Suita, Osaka 565-0871, Japan. [2]Department of Genetics, Graduate School of Medicine, Osaka University, 2-2 Yamadaoka, Suita, Osaka 565-0871, Japan. [3]Center for Frontier Oral Science, Graduate School of Dentistry, Osaka University, 1-8 Yamadaoka, Suita, Osaka 565-0871, Japan. [4]Department of Developmental Biology and Neurosciences, Graduate School of Life Sciences, Tohoku University, Aobayama, Aoba-ku, Sendai, Miyagi 980-8578, Japan.

*Authors for correspondence (takenoda@dent.osaka-u.ac.jp; tamyoshi@fbs.osaka-u.ac.jp)

K.I., 0000-0001-8297-2273; T.N., 0000-0003-3581-7961; T.Y., 0000-0001-9787-3788

Received 1 August 2016; Accepted 17 August 2016

Mammalian Atg9A, the yeast Atg9 homolog, is the sole multi-spanning transmembrane protein among the core Atg proteins. Although the transmembrane domain of Atg9A is well conserved between yeast and mammals, its length and amino acid sequence outside of this domain are not well conserved (Noda et al., 2000; Young et al., 2006). In mammalian cells, Atg9A mainly localizes to the trans-Golgi network (TGN) and also the endosomal system, and is reported to cycle between them though vesicle trafficking. Upon autophagy induction, a portion of Atg9A transiently localizes to the autophagic membranes (Orsi et al., 2012; Popovic and Dikic, 2014; Young et al., 2006). Recent studies have demonstrated that membrane trafficking pathways concerned with clathrin and/or adaptor proteins (Guo et al., 2012; Popovic and Dikic, 2014), Rab GTPases (Carlos Martín Zoppino et al., 2010; Itoh et al., 2008; Longatti et al., 2012) and the retromer complex (Zavodszky et al., 2014) are important for both proper Atg9A localization and autophagosome formation, indirectly suggesting that proper Atg9A trafficking is necessary for autophagy. However, the approach of manipulating general trafficking machinery used in the above studies means that it remains possible that defects in transport of molecules other than Atg9A itself causes autophagic inhibition. Therefore, we decided to pursue the significance of Atg9A trafficking in autophagy more directly by searching its intrinsic amino acid sequences for motifs required for its trafficking.

Transmembrane protein trafficking between the TGN, endosomes and the plasma membrane generally requires sorting motifs that are located within the cytoplasmic region of the protein (Bonifacino and Traub, 2003; Rohn et al., 2000). Such sorting motifs are usually recognized by adaptor protein (AP) complexes like AP-1 and AP-2, which sort and pack the transmembrane proteins into a transport vesicle as cargoes (Bonifacino and Traub, 2003). Hence, we attempted to investigate whether Atg9A has such sorting motifs, and succeeded to identify them in the N-terminal cytosolic stretch of Atg9A, which binds with AP-2. Mutation of these motifs brought about a trafficking defect of Atg9A, whereby Atg9A accumulated at the recycling endosomes, along with an autophagy defect. This combination of defects were also observed upon the knockdown of TRAPPC8, a specific subunit of the TRAPPIII complex. These findings prove that Atg9A trafficking from the recycling endosomes is a crucial step for the execution of both canonical and selective autophagy.

RESULTS

The N-terminal region of Atg9A is required for both autophagy and its Golgi localization

Atg9A is a membrane-spanning protein and its N- and C-terminal domains are extruded to the cytoplasm (Young et al., 2006). To explore the function of these cytoplasmic regions, we made a series of truncation mutants of Atg9A tagged with GFP at the C-terminus (Fig. S1A), and then stably expressed them in Atg9A-knockout

Journal of Cell Science (2016) 129, 3781-3791 doi:10.1242/jcs.196196

(KO) mouse embryonic fibroblast (MEF) cells. Compared to the wild-type (WT)-MEFs, Atg9A-KO MEFs showed a significantly lower number of autophagosomes, as visualized by immunostaining of LC3B proteins (also known as MAP1LC3 proteins; hereafter referred to collectively as LC3), an autophagosome marker (Kabeya et al., 2000; Saitoh et al., 2009), under nutrient-starved conditions (Fig. 1A). The deficiency was completely rescued by the stable expression of Atg9A-WT in Atg9A-KO MEFs (Fig. 1A). Whereas expression of C-terminal deletion mutants in Atg9A-KO MEFs completely restored the autophagic activity (Fig. S1B), cells expressing N-terminal deletion mutants showed defects in LC3 puncta formation. Cells expressing the ΔN(1-36) mutant of Atg9 had significantly fewer numbers of LC3 puncta under nutrient-starved conditions (Figs 1A and 2A). These results were also confirmed by another autophagy assay called the autophagic flux assay (Tanida et al., 2005). The lipidated form of LC3 (LC3-II) is degraded in autolysosomes, thus the level of LC3-II significantly increases in autophagy-competent cells upon treatment with Bafilomycin A1, which inhibits autophagosome and lysosome fusion. In contrast to the Atg9A-WT cells, accumulation of LC3-II was significantly blocked in Atg9A-KO MEFs expressing the ΔN (1-36) mutant (Fig. 1B). Thus, the N-terminal region (amino acids 1–36) in Atg9A is important for the role of Atg9A in autophagosome formation.

Next, we examined the localization of Atg9A mutant proteins. As previously reported, full-length Atg9A–GFP showed colocalization with the Golgi marker GM130 (also known as GOLGA2) (Fig. 1C) (Young et al., 2006). Deleting the C-terminal stretch did not affect Atg9A localization (Fig. S1C); by contrast, the N-terminal truncated mutant ΔN(1-12), and more severely with ΔN(1-36), did not show Golgi localization (Fig. 1C). Further deletion of the N- or C-terminal domain meant the protein failed to be expressed (data not shown). These results suggest that the N-terminal region (1–36) in Atg9A has a role in both autophagy and the correct localization of the protein.

Sorting motifs at the N-terminus of Atg9A are required for autophagy

We further characterized the N-terminal region of Atg9A. We noticed that the N-terminal region (1–36) of Atg9A has three putative sorting motifs as follows (Fig. 2A): (1) a di-acidic motif (residues 5–7) (DxE, where x represents any amino acid), (2) a tyrosine-based motif (residues 8–11) (YxxΦ, where Φ represents a bulky hydrophobic group), and (3) a di-leucine-based sorting motif (residues 22–27) [(D/E)xxxL(L/I/M/V) or D/ExxLL]. The di-acidic motif is recognized by Sec24, which functions in endoplasmic reticulum (ER) export (Nishimura and Balch, 1997), and both the tyrosine-based and di-leucine-based sorting motifs are recognized by the adaptor protein (AP), which functions in post-Golgi trafficking (Bonifacino and Traub, 2003), and are also recognized by Sec24 (Barlowe, 2003). Each sorting motif was replaced with alanine residues and expressed in Atg9A-KO MEFs, and their effects were then observed. The strongest defect in autophagosome formation was found when both the tyrosine-based and di-leucine-based sorting motifs (ΔYQRL+ΔLLV) were mutated (Fig. 2B). Consistent with this result, in the ΔYQRL+ΔLLV mutant, the LC3-II flux was significantly blocked (Fig. 2C), and degradation of p62 (also known as SQSTM1), a selective cargo protein of autophagy, was severely defected (Fig. S2A).

We next assessed whether the phenotypes of the ΔYQRL+ΔLLV mutant could be rescued by ectopically adding a sorting motif (+YQRL) or four alanine residues (+4Ala), as a control, at its N-terminus (Fig. 2A). The defects in autophagosome formation of the ΔYQRL+ΔLLV mutant was recovered by the external addition of YQRL motif, but not with the four alanine residues (Fig. 2D). These results demonstrate that the sorting motifs of Atg9A are required for its function in autophagy.

The sorting motifs are required for Atg9A trafficking from the recycling endosomes

Next, we observed the localization of the Atg9A mutants to see the function of these sorting motifs in its trafficking. Whereas mutation in the di-acidic motif did not affect the localization, mutation in either the tyrosine-based motif or di-leucine-based sorting motif decreased Atg9A localization on the Golgi, and instead the protein became dispersed within the cytosol as dot-like structures. Double mutation (ΔYQRL+ΔLLV) diminished the Golgi localization the most under nutrient-rich conditions (Fig. 3A). The decreased Golgi localization of the ΔYQRL+ ΔLLV mutant was recovered upon the addition of the YQRL motif at N-terminus of the mutant, but not with four alanine residues (Fig. 3B). These results show that the Golgi localization of Atg9A depends on the sorting motifs.

It could have been possible that localization change of the Atg9A mutants was caused by a defect in exiting from the ER because the tyrosine-based and di-leucine-based sorting motifs also work as an ER export signal (Barlowe, 2003). However, this was not the case because the Golgi form of *N*-glycan modification on Atg9A was observed in all mutants (Fig. S3). Therefore, it would be expected that these Atg9A mutants would be localized at a post-Golgi compartment, and we next aimed to assess the intracellular localization where the trafficking of the Atg9A mutants halted. They did not accumulate at the autophagosome formation sites, because they did not colocalize with the WIPI2 and Atg16L1 markers for the autophagosome formation site (Fig. S2B). Instead, a noticeable amount of the Atg9A accumulated at the juxtanuclear region when the tyrosine-based motif and/or di-leucine-based sorting motif were impaired under nutrient-starved conditions (Fig. 3A). These accumulated structures colocalized well with a recycling endosome marker (Alexa-Fluor-568–transferrin), which was not seen in the WT (Fig. 4A; Fig. S4A). We quantified this phenotype and found that the ΔYQRL+ΔLLV mutant showed 54.3% colocalization, whereas only 7.9% was found in WT (Fig. S4C). The ΔYQRL+ΔLLV mutant no longer accumulated on the recycling endosomes when the sorting motif was ectopically added to the N-terminus of this mutant (Fig. 4A, Fig. S4B). These results indicate that Atg9A depends on the sorting motifs to be transported from the recycling endosomes.

Atg9A sorting motifs interact with AP-2

The above results prompted us to further explore the adaptor proteins(s) that interact with the identified sorting motifs. So far there are two past studies about the adaptor proteins potentially involved in Atg9A trafficking, AP-1 and AP-2 (Guo et al., 2012; Popovic and Dikic, 2014). We therefore examined whether either of them was associated with the sorting motif by pulldown experiments. We found that we could successfully pulldown the AP-2 subunit adaptin α together with Atg9A–GFP, but not the AP-1 subunit adaptin γ, at least in our experimental system (ATG9A KO MEFs expressing functional Atg9A–GFP) (Fig. 4B). Importantly, the ΔYQRL+ΔLLV mutant Atg9A–GFP pulled down significantly less AP-2 than wild-type Atg9A (Fig. 4B). Thus, AP-2 is most likely to be the adaptor protein, at least in the sorting step where the sorting motif is involved.

Journal of Cell Science (2016) 129, 3781-3791 doi:10.1242/jcs.196196

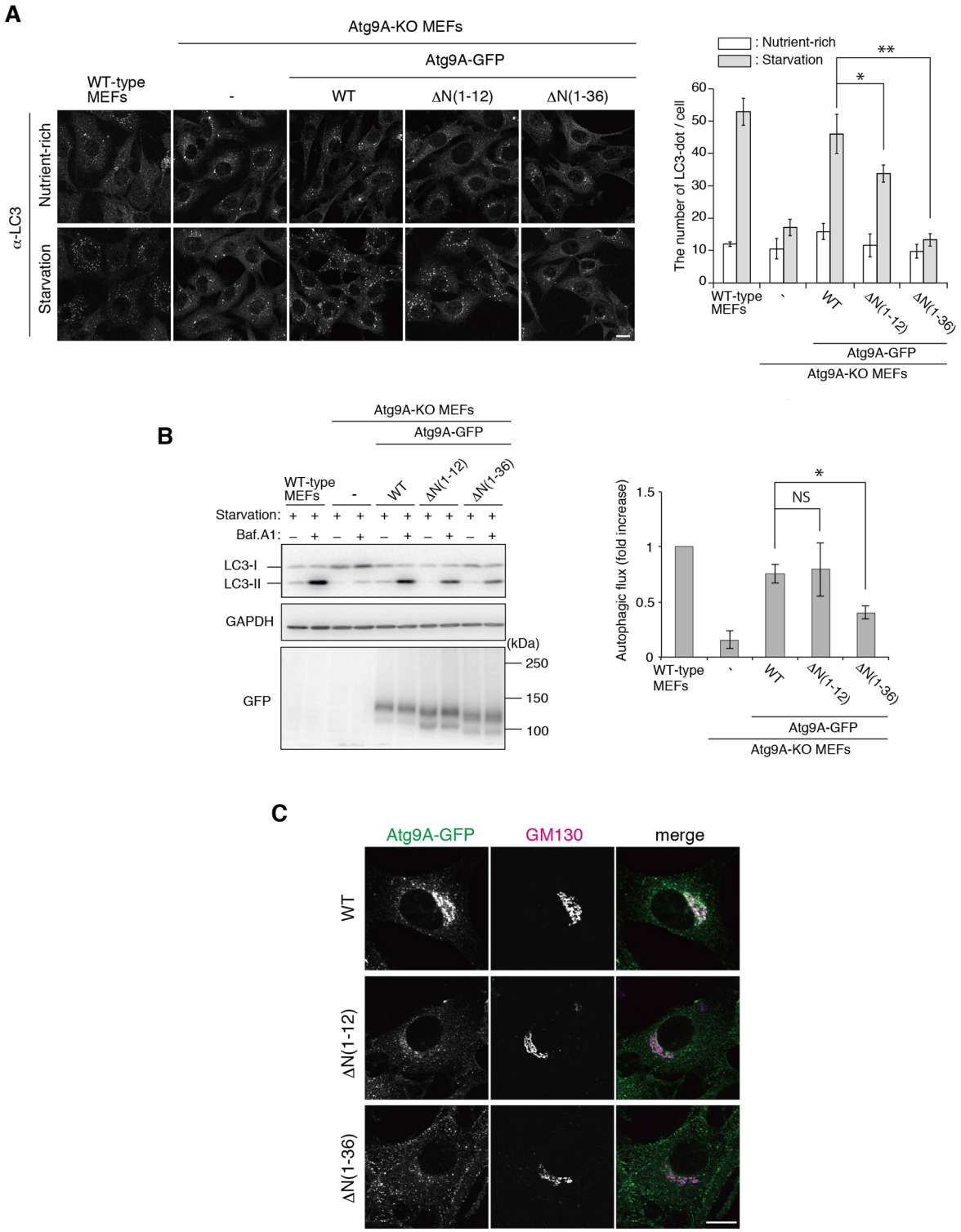

Fig. 1. The N-terminal region of Atg9A is required for autophagy and its Golgi localization. (A) Wild-type (WT) or Atg9A-KO MEFs stably expressing the indicated Atg9A constructs were cultured in growth medium (nutrient-rich) or EBSS (starvation) for 1 h, and then analyzed by immunocytochemistry for LC3, an autophagosome marker protein. Although Atg9A is essential for autophagosome formation, Atg9A-KO MEFs still show LC3-dot-like structures under the both nutrient-rich and nutrient-starved conditions, indicating that some LC3-positive structures are not autophagosomes (Saitoh et al., 2009). Thus, the number of LC3 puncta in Atg9A-KO MEFs is an overestimation of the number of autophagosomes. The number of LC3 puncta in each cell was counted for more than 30 cells. The mean±s.d. is shown for three independent experiments. *P<0.05; **P<0.01 (two-tailed paired Student's t-test). Scale bar: 20 µm. (B) Wild-type or Atg9A-KO MEFs stably expressing the indicated constructs were cultured in EBSS (starvation) for 4 h without or with 125 nM Bafilomycin A1 (Baf.A1), and subjected to western blotting using the indicated antibodies. The graph indicates the fold increase for the difference in LC3-II signal relative to GAPDH between the without and with Bafilomycin A1 conditions, indicative of autophagic flux. LC3-I, soluble form of LC3. The mean±s.d. is shown for three independent experiments. *P<0.05; NS, not significant (two-tailed paired Student's t-test). (C) Atg9A-KO MEFs stably expressing the indicated constructs were fixed, immunostained with anti-GM130 antibody and then observed by fluorescence microscopy. Scale bar: 20 µm.

Journal of Cell Science (2016) 129, 3781-3791 doi:10.1242/jcs.196196

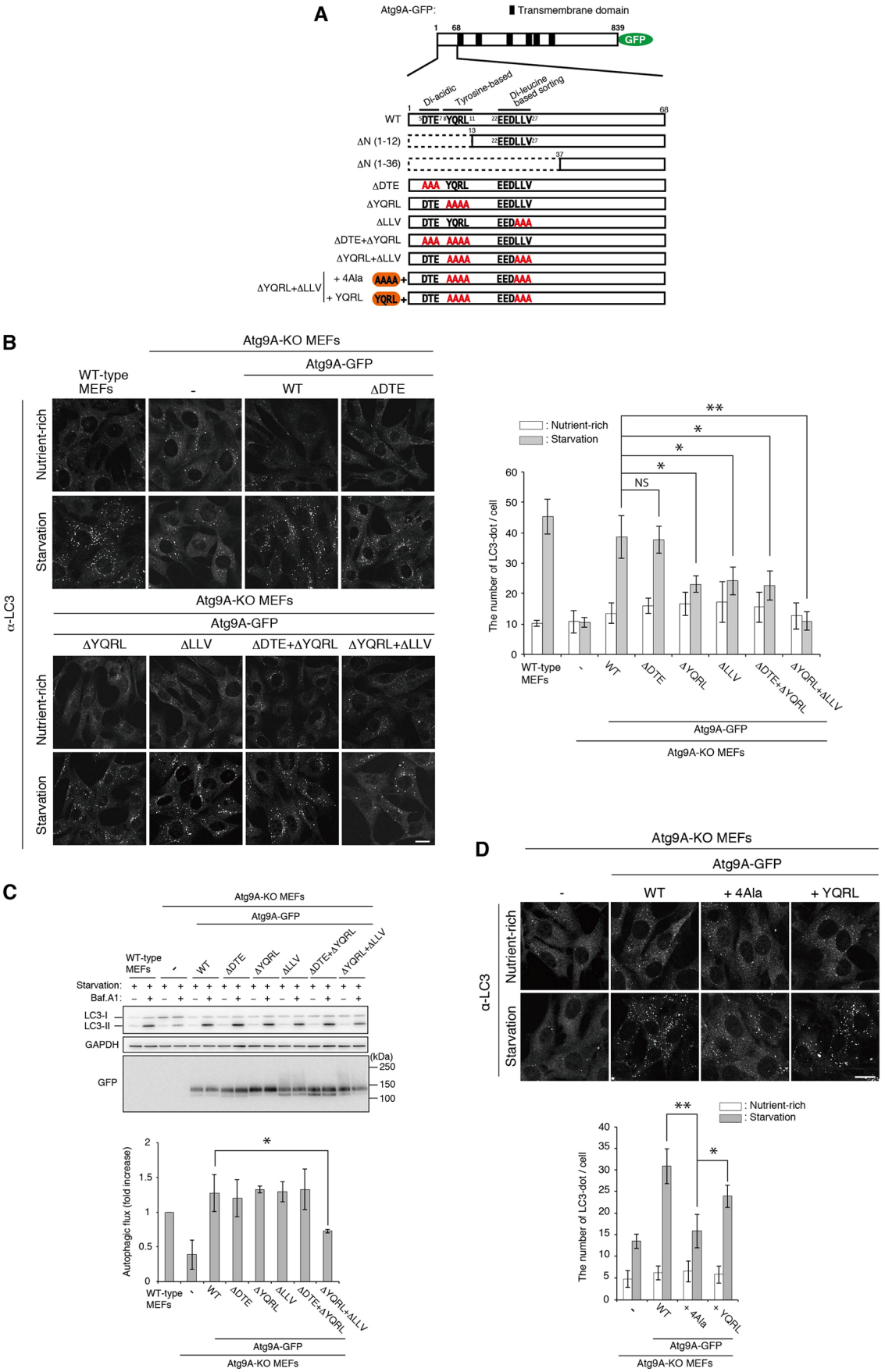

Fig. 2. See next page for legend.

Journal of Cell Science

Journal of Cell Science (2016) 129, 3781-3791 doi:10.1242/jcs.196196

Fig. 2. The tyrosine-based and di-leucine-based sorting motifs are required for starvation-induced autophagy. (A) Schematic diagram of wild-type (WT) Atg9A and its mutants used in the current study. Mouse Atg9A has three putative sorting motifs: a di-acidic motif, a tyrosine-based motif and a di-leucine-based sorting motif. (B) Wild-type or Atg9A-KO MEFs stably expressing the indicated constructs were cultured in growth medium (nutrient-rich) or EBSS (starvation) for 1 h, and then analyzed by immunocytochemistry for LC3. The number of LC3 puncta in each cell was counted for more than 30 cells. The mean±s.d. is shown for three independent experiments. **P*<0.05; ***P*<0.01; NS, not significant (two-tailed paired Student's *t*-test). Scale bar: 20 µm. (C) Wild-type or Atg9A-KO MEFs stably expressing the indicated constructs were cultured in EBSS (starvation) for 4 h without or with 125 nM Bafilomycin A1(Baf.A1), and subjected to western blotting using the indicated antibodies. The graph indicates the fold increase for the difference in the LC3-II signal relative to GAPDH between conditions without and with 125 nM Bafilomycin A1, indicative of autophagic flux. LC3-I, soluble form of LC3. The mean±s.d. is shown for three independent experiments. **P*<0.05 (two-tailed paired Student's *t*-test). (D) Atg9A-KO MEFs stably expressing the indicated constructs were cultured in growth medium (nutrient-rich) or EBSS (starvation) for 1 h, then analyzed by immunocytochemistry for LC3. The number of LC3 puncta in each cell was counted for more than 50 cells. The mean±s.d. is shown for three independent experiments. **P*<0.05; ***P*<0.01 (two-tailed paired Student's *t*-test). Scale bar: 20 µm.

Atg9A accumulates in the recycling endosomes upon TRAPPC8 knockdown, which also causes defects in autophagy

We further extended our study to strengthen the importance of Atg9A trafficking in autophagy by independent means. Recently, we have reported that the autophagy defect caused by the *trs85* mutant in yeast is due to a defect in yeast Atg9 trafficking from the endosome to the Golgi (Shirahama-Noda et al., 2013). Trs85 is a specific subunit of the TRAPPIII complex, a guanine-nucleotide exchange factor for Ypt1 (a Rab1 homolog), and functions as a vesicle-tethering complex, mediating general retrograde trafficking from endosomes to the Golgi (Lynch-Day et al., 2010; Shirahama-Noda et al., 2013). Interestingly, it has been reported that knockdown of TRAPPC8, a mammalian homolog of Trs85, blocks both retrograde transport of Shiga toxin from the endosome to the ER (Kampmann et al., 2013) and autophagy (Behrends et al., 2010). Therefore, we examined the possibility that TRAPPC8 knockdown mediated by small interfering RNA (siRNA) affects Atg9A trafficking. Although Atg9A was only minimally colocalized with the recycling endosome marker (Alexa-Fluor-568–transferrin) in control siRNA-transfected cells, it was clearly colocalized with this marker in TRAPPC8-siRNA-transfected cells (Fig. 5A), indicating that Atg9A was trapped on the recycling endosomes upon TRAPPC8 knockdown. We could also reproduce the results from the previous report showing that knockdown of TRAPPC8 severely blocked autophagosome formation (Fig. 5B; Behrends et al., 2010). These observations support the idea that Atg9A trafficking through the recycling endosomes is required for autophagosome formation.

Sorting motifs at the N-terminus of Atg9A are also required for selective autophagy against *Salmonella*

We finally asked whether the sorting motifs in Atg9A are involved in selective autophagy as well as starvation-induced nonselective autophagy. Autophagy targets intracellular-invading *Salmonella* and suppresses their growth inside cells (Birmingham et al., 2006). In this process, Atg9A is recruited to the intracellular *Salmonella* that are positive for ubiquitin before eventually dissociating from them (Fujita et al., 2013; Kageyama et al., 2011). First, we assessed whether the sorting motifs are required for the recruitment of Atg9A to the bacteria. To this purpose, we calculated the percentage of Atg9A recruitment to ubiquitin-positive *Salmonella*. We used FAK-family-interacting protein of 200 kDa (FIP200)-KO MEFs (FIP200 is also known as RB1CC1), in which Atg9A is targeted to the Salmonella as normal but cannot dissociate from them; thus, Atg9A-positive *Salmonella* accumulate in FIP200-KO MEFs compared to WT MEFs (Kageyama et al., 2011). The percentage of the ΔYQRL+ΔLLV mutant recruitment to *Salmonella* in these MEFs was significantly lower than that of Atg9A-WT (Fig. 6A), demonstrating that the sorting motifs were required for the recruitment of Atg9A to the *Salmonella*.

Next, we tested whether the sorting motifs were indispensable for the bacterial growth arrest. The number of *Salmonella* within the host cells was counted at the indicated time points. Atg9A-KO MEFs expressing Atg9A-WT suppressed *Salmonella* growth; however, Atg9A-KO MEFs expressing ΔYQRL+ΔLLV allowed *Salmonella* to grow (Fig. 6B), indicating that the sorting motifs are required for the function of Atg9A in selective autophagy. Taken together, we conclude that the sorting motifs of Atg9A are indispensable for selective autophagy as well as canonical autophagy.

DISCUSSION

In this study, we have succeeded in identifying the intrinsic Atg9A sorting motif (tyrosine-based and di-leucine-based sorting motif) at its N-terminal cytoplasmic region, which binds to AP-2. This motif is crucial for its proper localization and for autophagy. In contrast to previous studies showing that general membrane trafficking defects somehow lead to an autophagy defect, which was analyzed by several methods such as knockdown of membrane trafficking machineries (Guo et al., 2012; Itoh et al., 2008; Longatti et al., 2012; Popovic and Dikic, 2014; Takahashi et al., 2011; Webber and Tooze, 2010), drugs (Köchl et al., 2006; Puri et al., 2013) and temperature block (Puri et al., 2013) methods, our findings directly clarify that Atg9A trafficking itself is prerequisite for autophagy. Our results do not necessarily exclude the possibility that some other cargoes of general membrane trafficking are also required for autophagy. However so far, there are only two transmembrane proteins that have been shown to be required for autophagy, Atg9A and VMP1, and VMP1 is an ER-resident protein (Ropolo et al., 2007). So at this stage, we propose that Atg9A is the sole known cargo protein under the control of general membrane trafficking that is essential for autophagy.

The Atg9A mutant lacking both the tyrosine-based and di-leucine-based sorting motifs exhibited a decreased Golgi localization, and abnormal accumulation on the recycling endosomes under nutrient-starved conditions (Fig. 4A). The adaptor protein AP-2 would be expected to directly bind to this motif and direct Atg9A to the transport vesicle destined to the next destination, the Golgi and possibly, successively, to the autophagosome (Fig. 7A). This also suggests that nutrient starvation conditions lead to the rerouting of Atg9A trafficking so that it passes through the recycling endosomes.

The importance of exit of Atg9A from the recycling endosomes was also supported by the other experiment, knockdown of TRAPPC8. Resulting accumulation of Atg9A on the recycling endosomes indicates that TRAPPC8 is involved in the retrograde trafficking of Atg9A from the recycling endosomes to the Golgi. This idea is consistent with a recent paper from the laboratory of Sharon Tooze reporting that TRAPPIII complex can bind with TBC1D14 at the recycling endosomes, where Rab1 is activated, and can mediate membrane trafficking from endosomes to the Golgi (Lamb et al., 2015). They also showed that TBC1D14

Journal of Cell Science (2016) 129, 3781-3791 doi:10.1242/jcs.196196

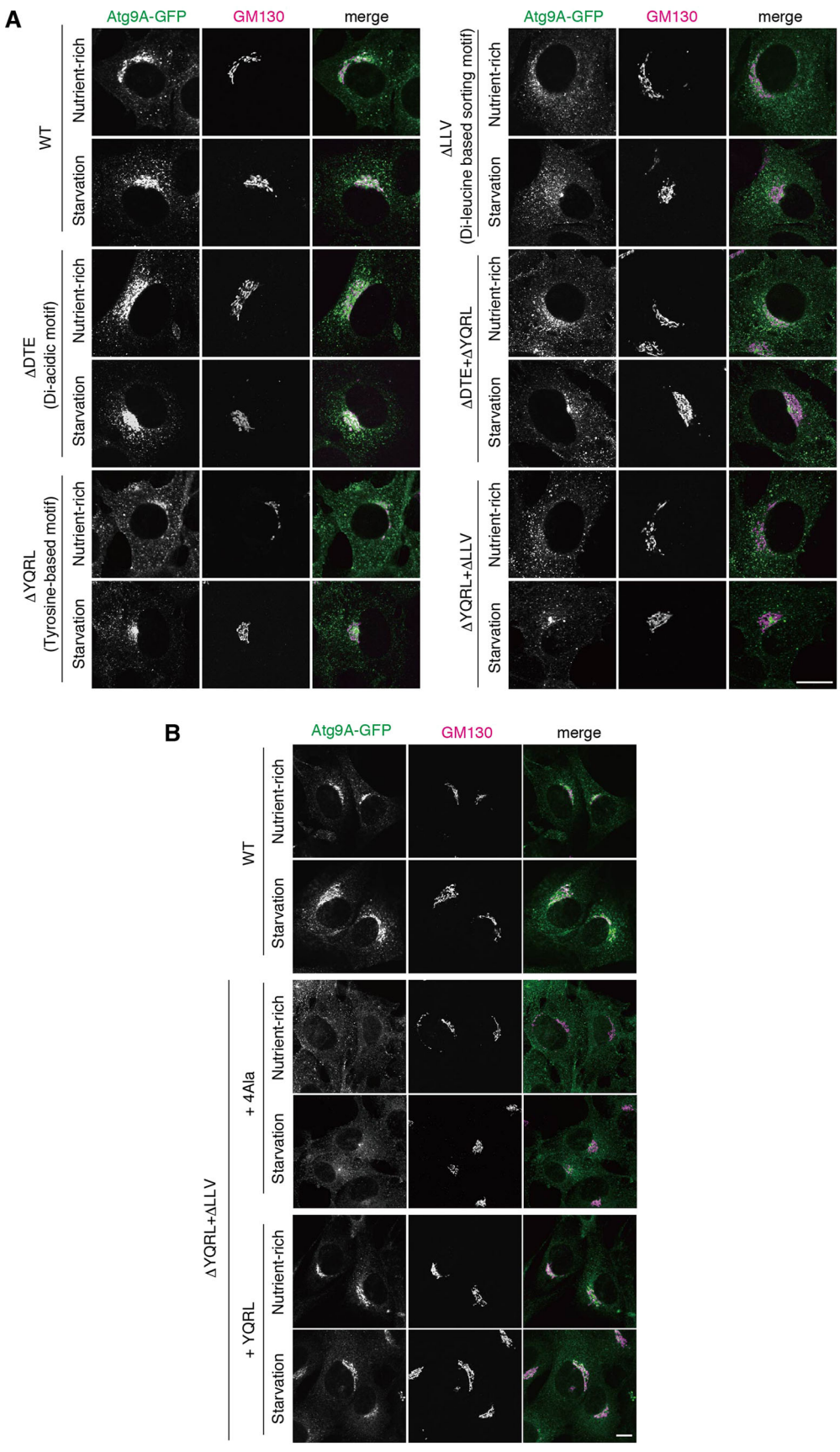

Fig. 3. The sorting motifs of Atg9A are crucial for its Golgi localization. (A,B) Atg9A-KO MEFs stably expressing the indicated constructs were cultured in growth medium (nutrient-rich) or EBSS (starvation) for 1 h, and then analyzed by immunocytochemistry for GM130 (a Golgi marker). Scale bars: 20 µm.

Journal of Cell Science (2016) 129, 3781-3791 doi:10.1242/jcs.196196

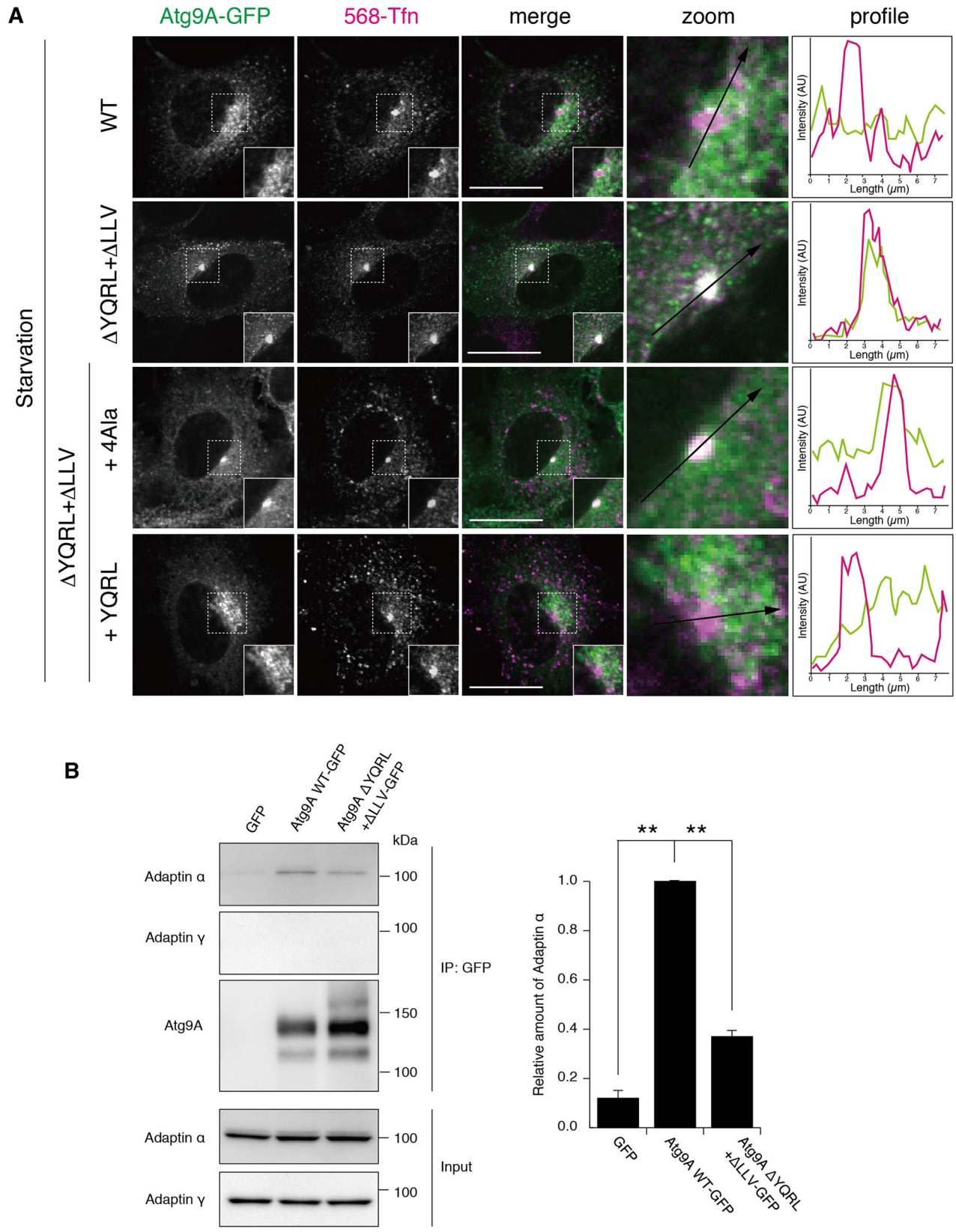

Fig. 4. Binding of AP-2 with the sorting motifs in Atg9A is required for Atg9A trafficking through the recycling endosomes. (A) Atg9A-KO MEFs stably expressing the indicated constructs were cultured in EBSS (starvation) with 10 µg/ml Alexa-Fluor-568–transferrin (586-Tfn) for 1 h, fixed, and then observed by fluorescence microscopy. A linescan profile through the sectioned indicated by the arrow in the zoom image is shown on the right. Scale bars: 20 µm. (B) Atg9A-KO MEFs stably expressing the indicated proteins were lysed and immunoprecipitated with anti-GFP antibody. The immunoprecipitated (IP) materials were western blotted with antibodies against adaptin α and adaptin β. The graph indicates a quantification of the amount of adaptin α in immunoprecipitation samples. The mean±s.d. is shown for three independent experiments. $^{**}P<0.001$ (two-tailed paired Student's *t*-test).

Journal of Cell Science (2016) 129, 3781-3791 doi:10.1242/jcs.196196

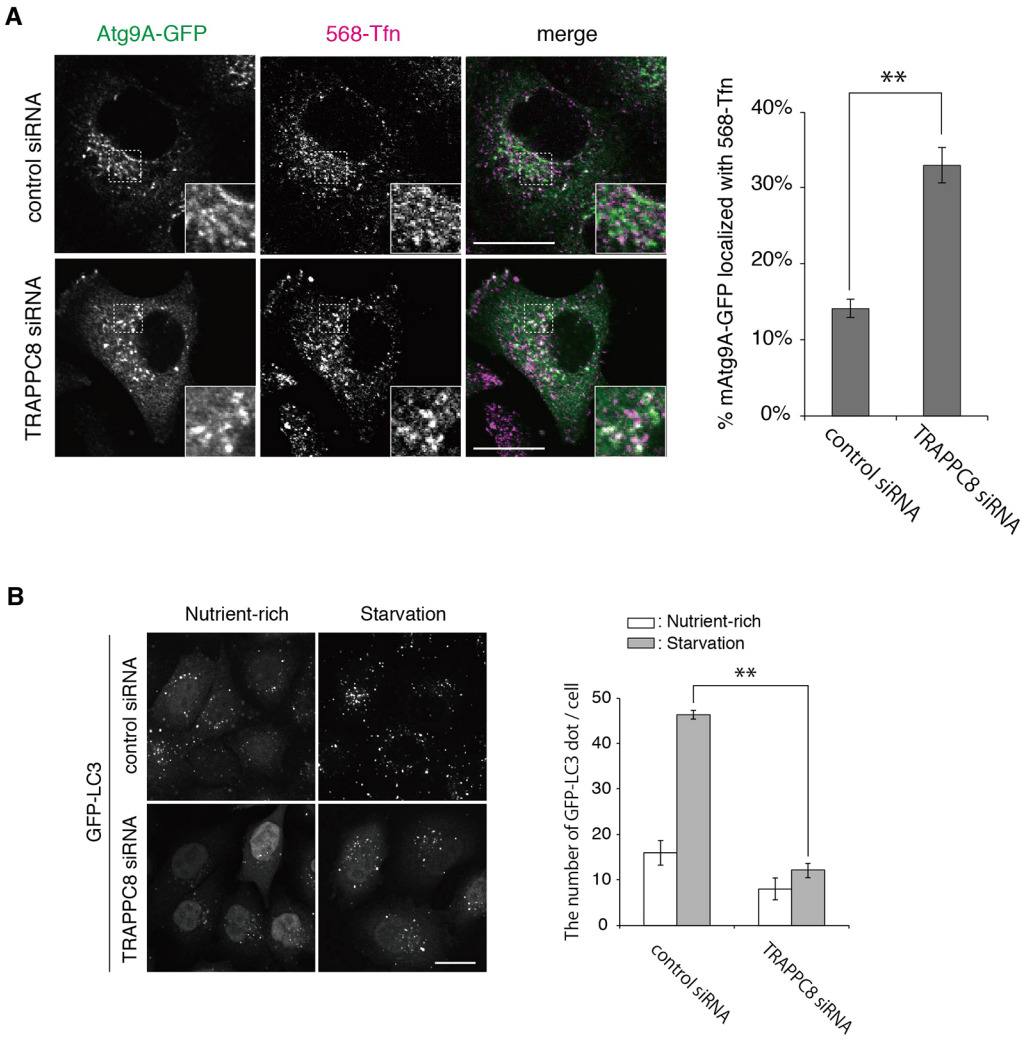

Fig. 5. TRAPPC8 is required for Atg9A trafficking through the recycling endosomes and autophagy. (A) HeLa Kyoto cells stably expressing Atg9A–GFP were treated with siRNA targeting a control (luciferase) or *TRAPPC8*. At 72 h after transfection, the cells were incubated with DMEM with 10 µg/ml Alexa-Fluor-568–transferrin (586-Tfn) for 2 h, fixed, and then observed by fluorescence microscopy. The bar graph shows the percentage of Atg9A–GFP colocalized with the indicated marker. Percentage colocalization was determined by calculating the Manders' colocalization coefficient. The mean ±s.d. is shown for three independent experiments. $^{**}P<0.01$ (two-tailed paired Student's *t*-test). (B) HeLa Kyoto cells stably expressing GFP–LC3 were transfected with siRNA targeting control (luciferase) or *TRAPPC8*. At 72 h after transfection, the cells were cultured in growth medium (nutrient-rich) or EBSS (starvation) for 2 h, fixed, and then examined by fluorescence microscopy. The number of GFP–LC3 puncta in each cell was counted for more than 50 cells. The mean±s.d. is shown for three independent experiments. $^{**}P<0.01$ (two-tailed paired Student's *t*-test). Scale bar: 20 µm.

overexpression causes tubulation of the recycling endosomes and defects in the recycling pathway, suggesting that interaction between TBC1D14 and TRAPPIII complex is required for membrane trafficking from the recycling endosomes to the Golgi. Collectively, Atg9A trafficking from recycling endosomes is important for autophagosome formation [Fig. 7B, pathway (ii)]. This is in line with our previous report showing that in yeast the defect in endosome-to-Golgi trafficking leads to failure of yeast Atg9 arrival to autophagosome or PAS (preautophagosomal structure). Endosome-to-golgi trafficking, and possibly a shuttling between the endosome and the Golgi, could serve as a reservoir for yeast Atg9 protein, with a portion of the yeast Atg9 being delivered to PAS and autophagosome from there (Shirahama-Noda et al., 2013).

It has been suggested that the recycling endosome membrane is one of the membrane sources for autophagosome formation (Knævelsrud et al., 2013; Longatti et al., 2012; Orsi et al., 2012); thus, it might be possible that Atg9A could mediate the delivery of core nucleation factor(s) from the recycling endosomes to the autophagosome. However, a more plausible possibility revealed in this study is that delivery of Atg9A itself from the recycling endosomes to the Golgi, rather than some specific membrane lipid, is the crucial role of membrane trafficking during autophagy. However it is still possible that Atg9A recruits some unknown factors from the recycling endosomes to the autophagosome, and we need to decipher these possibilities in future study. We note that there is also a possibility that Atg9A reaches the forming autophagosome directly from the recycling endosomes [Fig. 7B, pathway (i)]. Canonical and selective autophagy share some common mechanisms and differences; however, the whole picture has not yet been clarified. Finding that Atg9A trafficking is indispensable for both types of autophagy is an important first step to fully understand the mechanisms. Our results establish that Atg9A trafficking itself is the reason that membrane trafficking is required in autophagy, and future study will give us more detailed understanding regarding the role of Atg9A.

MATERIALS AND METHODS

Plasmid constructions and virus productions

pENTR1A vector was purchased from Invitrogen. The pMRX-IRES-puro vector was kindly provided by Toshio Kitamura (University of Tokyo, Tokyo, Japan) (Morita et al., 2000). The DNA fragment containing attR1, ccdB, CmR and attR2 was PCR amplified from pAd/CMV/V5-DEST (Invitrogen) and digested with BglII-NotI. The fragment was subcloned into the BamHI-NotI sites of pMRX-IRES-puro (pMRX-IRES-puro-DEST). pEGFP-Atg9A was generously provided by Toshihiko Yamada (Hokkaido University, Hokkaido, Japan). pDsRed-KDEL was kindly provided by Eiji Morita (Hirosaki University, Hokkaido, Japan). EGFP was PCR amplified from pEGFP-N1 (Invitrogen) and digested with BglII-NotI. The fragment was subcloned into the BamHI-NotI sites of pENTR1A (pENTR1A-EGFP). Atg9A was PCR amplified from pEGFP-Atg9A and digested with EcoRI-

Journal of Cell Science (2016) 129, 3781-3791 doi:10.1242/jcs.196196

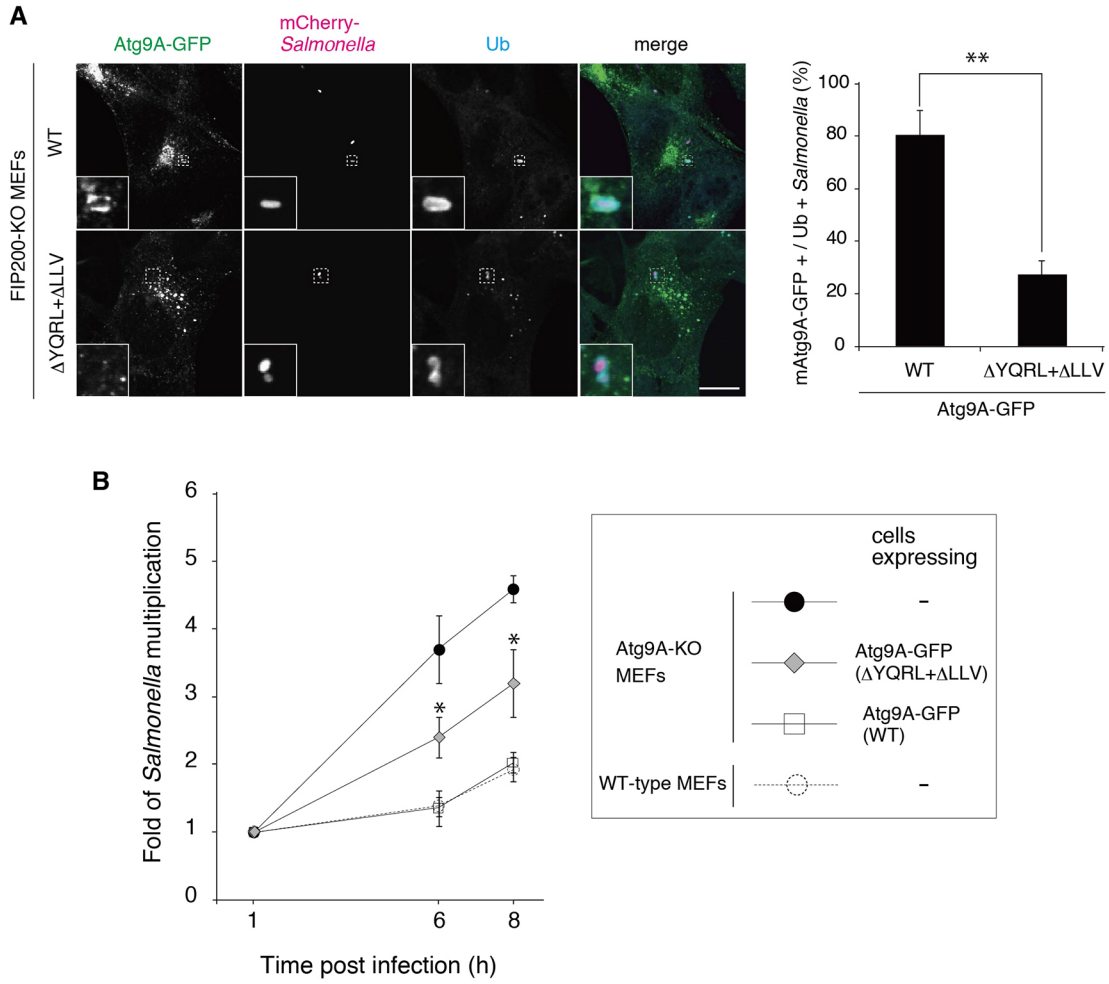

Fig. 6. The tyrosine-based and di-leucine-based sorting motifs of Atg9A are required for autophagy against *Salmonella*. (A) FIP200-KO MEFs stably expressing the indicated constructs were infected with *Salmonella* expressing mCherry (MOI=200) for 1 h, and then analyzed by immunocytochemistry for ubiquitin (Ub). The percentage of Atg9A-positive *Salmonella* as a proportion of ubiquitin-positive *Salmonella* was counted from fluorescence microscopy images. At least 50 bacteria were counted. The mean±s.d. is shown for three independent experiments. $^{**}P<0.01$ (two-tailed paired Student's *t*-test). Scale bar: 20 µm. (B) Wild-type (WT) or Atg9A-KO MEFs stably expressing the indicated constructs were infected with *Salmonella* expressing mCherry for 10 min at a MOI of 100. After infection, the cells were washed to remove extracellular *Salmonella* and incubated in DMEM containing gentamicin for the indicated time, fixed and then examined by fluorescence microscopy. The number of *Salmonella* in each cell was counted for more than 50 cells. The mean±s.d. is shown for three independent experiments. $^{*}P<0.05$ (two-tailed paired Student's *t*-test).

KpnI. The fragment was subcloned into the EcoRI-KpnI sites of pENTR1A-EGFP (pENTR1A-Atg9A-EGFP). Various Atg9A mutants were created from pENTR1A-Atg9A-EGFP with the QuikChange technique, including ΔN(1-12), ΔN(1-36), ΔC(799-839), ΔC(715-839), ΔC(672-839), ΔC(630-839), ΔC(585-839), ΔDTE, ΔYQRL, ΔLLV, ΔDTE+ΔYQRL and ΔYQRL +ΔLLV, and RXR (RXR construct was used in Fig. S3). pENTR1A-Atg9A-EGFP and pENTR1A-Atg9A-EGFP including various Atg9A mutation sequences were transferred into the pMRX-IRES-puro-DEST vector using an LR reaction. Recombinant retroviruses were prepared as previously described (Saitoh et al., 2003). Plat-E cells were generously provided by Toshio Kitamura (Morita et al., 2000).

Reagents and antibodies

The following antibodies were used: mouse monoclonal anti-GFP (1:2000, cat. no. 11814460001, Roche), mouse monoclonal anti-GM130 (1:1000, cat. no. 610822, BD), mouse monoclonal anti-p230 (1:1000, cat. no. 611280, BD), mouse monoclonal anti-TfR (1:500, cat. no. 13-6800, Invitrogen), mouse monoclonal anti-poly-ubiquitin (1:2000, cat. no. BML-PW8810, clone FK2; BIOMOL), mouse monoclonal anti-GAPDH (1:2000, cat. no. Mab314, Chemicon, Merck Millipore), mouse monoclonal anti-γ-adaptin (1:3000, cat. no. 610386, BD), rabbit polyclonal anti-LC3 (1:1000 for immunofluorescence, 1:2000 for western blotting, cat. no. PM036, MBL), rabbit polyclonal anti-p62 (1:1000, cat. no. PM045, MBL), rabbit polyclonal anti-EEA1 (1:100, cat. no. 2411S, Cell Signaling Technology), mouse monoclonal anti-α-adaptin (1:3000, cat. no. 610502, BD), rabbit polyclonal anti-Atg9 (1:500; cat no. PD042, MBL), rabbit polyclonal anti-Atg16L1 (1:500, cat. no. TMD-PH-AT16L, Cosmobio), rabbit polyclonal anti-WIPI-2 (1:1000, cat. no. SAB4200400, Sigma). Bafilomycin A1 was purchased from Sigma-Aldrich. Alexa-Fluor-568–transferrin was purchased from Invitrogen. Wheat germ agglutinin (WGA)-conjugated Alexa Fluor 568 was purchased from Invitrogen. Endo Hf was purchased from New England Biolabs. PNGaseF was purchased from New England Biolabs.

Immunofluorescence microscopy

Samples were fixed with 4% paraformaldehyde for 20 min, quenched with 50 mM NH_4Cl or phosphate-buffered saline (PBS), permeabilized with 50 µg/ml digitonin in PBS, blocked with 0.1% gelatin in PBS and then incubated with the indicated primary antibodies. After washing with PBS, the samples were incubated with secondary antibodies and mounted with Slow Fade Gold (Invitrogen). The microscopy images were taken using a FV1000 confocal laser-scanning microscope system equipped with a 60×1.40 NA oil immersion objective lens. Fluorochromes associated with

Journal of Cell Science (2016) 129, 3781-3791 doi:10.1242/jcs.196196

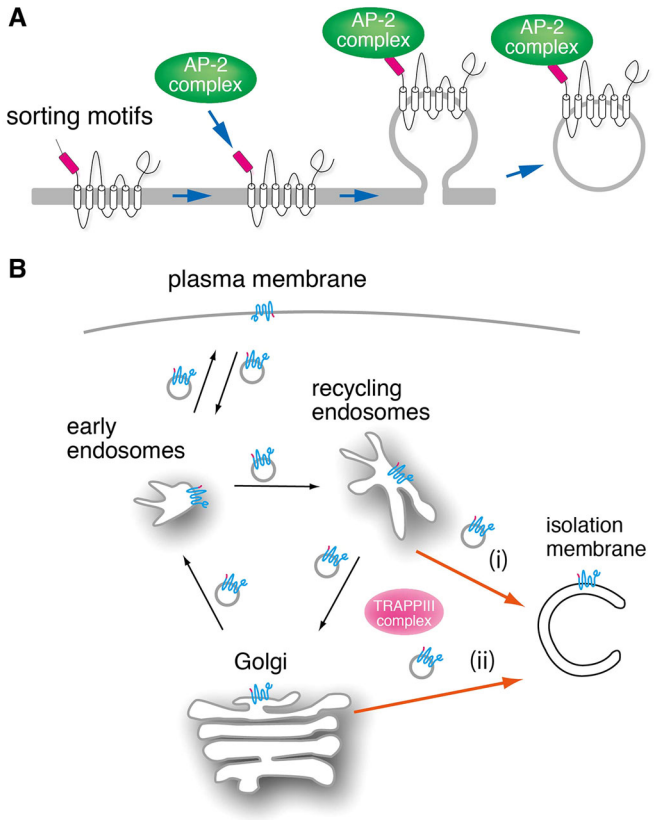

Fig. 7. Proposed models for Atg9A trafficking and autophagosome formation. (A) The adaptor protein, AP-2, directly binds to sorting motifs and drives the segregation of Atg9A into appropriate transport vesicles for distinct transport. (B) At the steady state, Atg9A cycles between the trans-Golgi network (TGN), the endosomal system and the plasma membrane through vesicle trafficking. Atg9A traffics to and from the recycling endosomes. Retrograde trafficking of this pathway depends on the sorting motifs in Atg9A and the TRAPPIII complex. Upon autophagy induction, a portion of Atg9A transiently localizes to the isolation membranes through (i) the recycling endosomes and/or (ii) the Golgi.

the secondary antibodies were conjugated to Alexa Fluor 568 or 647. Image acquisition software Fluoview (Olympus) was used. The images were adjusted using Photoshop CS4 software (Adobe). The number of LC3 particles was analyzed by G-Count (G-Angstrom).

Cell culture and transfection

MEFs, HeLa Kyoto and Plat-E cells were cultured in Dulbecco's modified Eagle's medium (DMEM D6429; Sigma-Aldrich) containing 10% fetal bovine serum (FBS), 5 U/ml penicillin, and 50 U/ml streptomycin at 37°C with 5% CO_2 (denoted growth medium). For nutrient starvation, cells were cultured in EBSS (Sigma-Aldrich). Transient transfection was carried out using Lipofectamine 2000 reagent (Invitrogen) according to the manufacturer's protocol.

Western blotting

Cells were lysed in ice-cold RIPA buffer (50 mM Tris-HCl pH 8.0, 150 mM NaCl, 1% w/v Triton X-100, 0.1% SDS, 0.5% sodium deoxycholate) containing protease inhibitor cocktail (Roche) and 1 mM phenylmethylsulfonyl fluoride. Lysates were mixed with 5× SDS sample buffer and heated at 60°C for 5 min. Samples were analyzed by SDS-PAGE and transferred to polyvinylidene difluoride membrane. The membranes were blocked with 1% skim milk in 0.1% Tween 20 in Tris-buffered saline (TBS) and incubated with primary antibodies. Immunoreactive bands were detected using horseradish peroxidase (HRP)-conjugated secondary antibodies (Jackson ImmunoResearch Laboratories, West Grove, PA), Luminata Forte (Merck Millopore) and a chemiluminescence detector (LAS-3000, Fujifilm).

Bacterial infection

Salmonella enterica serovar Typhimurium SR-11 x3181 harboring the pBR-mCherry plasmid were grown overnight at 37°C, and then subcultured at 1:33 for 3 h in LB without antibiotics. The bacterial inocula were prepared by pelleting at 10,000 ***g*** for 2 min, and were then added to host cells at a multiplicity of infection (MOI) of 100–200 at 37°C with 5% CO_2.

RNA interference

siRNA duplex oligomers were designed as follows: 5′-UCGAAGUAUU-CCGCGUACG-3′ (luciferase), 5′-GCACAUUGCUUUAUAAACA-3′ (TRAPPC8). A total of 20 nM siRNA was introduced to cells using RNAiMAX (Invitrogen) according to the manufacturer's instructions.

Immunoprecipitation

MEFs stably expressing GFP, Atg9A-WT–GFP or Atg9A-ΔYQRL+ΔLLV–GFP were lysed in buffer containing 20 mM CHAPS (Dojindo), 125 mM NaCl, 50 mM Tris-HCl pH 7.5 and complete protease inhibitor cocktail (Roche). Lysates were cleared by centrifugation at 20,400 ***g*** for 10 min. The supernatant was incubated with GFP-Trap_M beads (Chromotek, gtm-20) at 4°C for 3 h. The beads were washed three times with lysis buffer and eluted with 1× sample buffer (2% SDS, 100 mM DTT, 60 mM Tris-HCl pH 6.8, 10% glycerol, 0.001% Bromophenol Blue). After boiling for 5 min, the samples were subjected to western blotting. Quantification of band intensity was performed using the IMAGEJ software (National Institutes of Health, Bethesda, MD, USA).

Acknowledgements

The authors would like to thank T. Yamada for pEGFP-Atg9A vector; E. Morita for pDsRed-KDEL; T. Kitamura for PLAT-E cells and pMX-puro vector; and all of Yoshimori-Lab member for helpful discussion.

Competing interests

The authors declare no competing or financial interests.

Author contributions

K.I. performed most of the experiments. Y.T. analyzed the deletion mutant of Atg9A. F.H. helped a knock down experiments of TRAPPC8 and performed IP experiment with Y.A. N.F. and M.H. contributed valuable discussion. T.Y. and T.N. designed the study and wrote the manuscript.

Funding

This work was supported by Special Coordination Funds for Promoting Science and Technology of the Ministry of Education, Culture, Sports, Science, and Technology (MEXT) of Japan [grant numbers 25111002 to T.Y., and 26111512 and 25293372 to T.N.].

Supplementary information

Supplementary information available online at
http://jcs.biologists.org/lookup/doi/10.1242/jcs.196196.supplemental

References

Barlowe, C. (2003). Signals for COPII-dependent export from the ER: what's the ticket out? *Trends Cell Biol.* **13**, 295-300.

Behrends, C., Sowa, M. E., Gygi, S. P. and Harper, J. W. (2010). Network organization of the human autophagy system. *Nature* **466**, 68-76.

Birmingham, C. L., Smith, A. C., Bakowski, M. A., Yoshimori, T. and Brumell, J. H. (2006). Autophagy controls salmonella infection in response to damage to the salmonella-containing vacuole. *J. Biol. Chem.* **281**, 11374-11383.

Bonifacino, J. S. and Traub, L. M. (2003). Signals for sorting of transmembrane proteins to endosomes and lysosomes. *Annu. Rev. Biochem.* **72**, 395-447.

Carlos Martín Zoppino, F., Damián Militello, R., Slavin, I., Álvarez, C. and Colombo, M. I. (2010). Autophagosome formation depends on the small GTPase Rab1 and functional ER exit sites. *Traffic* **11**, 1246-1261.

Fujita, N., Morita, E., Itoh, T., Tanaka, A., Nakaoka, M., Osada, Y., Umemoto, T., Saitoh, T., Nakatogawa, H., Kobayashi, S. et al. (2013). Recruitment of the autophagic machinery to endosomes during infection is mediated by ubiquitin. *J. Cell Biol.* **203**, 115-128.

Guo, Y., Chang, C., Huang, R., Liu, B., Bao, L. and Liu, W. (2012). AP1 is essential for generation of autophagosomes from the trans-Golgi network. *J. Cell Sci.* **125**, 1706-1715.

Itoh, T., Fujita, N., Kanno, E., Yamamoto, A., Yoshimori, T. and Fukuda, M. (2008). Golgi-resident Small GTPase Rab33B Interacts with Atg16L and Modulates Autophagosome Formation. *Mol. Biol. Cell* **19**, 2916-2925.

Kabeya, Y., Mizushima, N., Ueno, T., Yamamoto, A., Kirisako, T., Noda, T., Kominami, E., Ohsumi, Y. and Yoshimori, T. (2000). LC3, a mammalian homologue of yeast Apg8p, is localized in autophagosome membranes after processing. *EMBO J.* **19**, 5720-5728.

Kageyama, S., Omori, H., Saitoh, T., Sone, T., Guan, J.-L., Akira, S., Imamoto, F., Noda, T. and Yoshimori, T. (2011). The LC3 recruitment mechanism is separate from Atg9L1-dependent membrane formation in the autophagic response against Salmonella. *Mol. Biol. Cell* **22**, 2290-2300.

Kampmann, M., Bassik, M. C. and Weissman, J. S. (2013). Integrated platform for genome-wide screening and construction of high-density genetic interaction maps in mammalian cells. *Proc. Natl. Acad. Sci. USA* **110**, E2317-E2326.

Kawabata, T. and Yoshimori, T. (2016). Beyond starvation: an update on the autophagic machinery and its functions. *J. Mol. Cell. Cardiol.* **95**, 2-10.

Knævelsrud, H., Søreng, K., Raiborg, C., Håberg, K., Rasmuson, F., Brech, A., Liestøl, K., Rusten, T. E., Stenmark, H., Neufeld, T. P. et al. (2013). Membrane remodeling by the PX-BAR protein SNX18 promotes autophagosome formation. *J. Cell Biol.* **202**, 331-349.

Köchl, R., Hu, X. W., Chan, E. Y. W. and Tooze, S. A. (2006). Microtubules Facilitate Autophagosome Formation and Fusion of Autophagosomes with Endosomes. *Traffic* **7**, 129-145.

Lamb, C. A., Nühlen, S., Judith, D., Frith, D., Snijders, A. P., Behrends, C. and Tooze, S. A. (2015). TBC1D14 regulates autophagy via the TRAPP complex and ATG9 traffic. *EMBO J.* **35**, 281-301.

Longatti, A., Lamb, C. A., Razi, M., Yoshimura, S.-I., Barr, F. A. and Tooze, S. A. (2012). TBC1D14 regulates autophagosome formation via Rab11- and ULK1-positive recycling endosomes. *J. Cell Biol.* **197**, 659-675.

Lynch-Day, M. A., Bhandari, D., Menon, S., Huang, J., Cai, H., Bartholomew, C. R., Brumell, J. H., Ferro-Novick, S. and Klionsky, D. J. (2010). Trs85 directs a Ypt1 GEF, TRAPPIII, to the phagophore to promote autophagy. *Proc. Natl. Acad. Sci. USA* **107**, 7811-7816.

Morita, S., Kojima, T. and Kitamura, T. (2000). Plat-E: an efficient and stable system for transient packaging of retroviruses. *Gene Ther.* **7**, 1063-1066.

Nakatogawa, H., Suzuki, K., Kamada, Y. and Ohsumi, Y. (2009). Dynamics and diversity in autophagy mechanisms: lessons from yeast. *Nat. Rev. Mol. Cell Biol.* **10**, 458-467.

Nishimura, N. and Balch, W. E. (1997). A di-acidic signal required for selective export from the endoplasmic reticulum. *Science* **277**, 556-558.

Noda, T., Kim, J., Huang, W.-P., Baba, M., Tokunaga, C., Ohsumi, Y. and Klionsky, D. J. (2000). Apg9p/Cvt7p is an integral membrane protein required for transport vesicle formation in the Cvt and autophagy pathways. *J. Cell Biol.* **148**, 465-480.

Orsi, A., Razi, M., Dooley, H. C., Robinson, D., Weston, A. E., Collinson, L. M. and Tooze, S. A. (2012). Dynamic and transient interactions of Atg9 with autophagosomes, but not membrane integration, are required for autophagy. *Mol. Biol. Cell* **23**, 1860-1873.

Popovic, D. and Dikic, I. (2014). TBC1D5 and the AP2 complex regulate ATG9 trafficking and initiation of autophagy. *EMBO Rep.* **15**, 392-401.

Puri, C., Renna, M., Bento, C. F., Moreau, K. and Rubinsztein, D. C. (2013). Diverse autophagosome membrane sources coalesce in recycling endosomes. *Cell* **154**, 1285-1299.

Rohn, W. M., Rouille, Y., Waguri, S. and Hoflack, B. (2000). Bi-directional trafficking between the trans-Golgi network and the endosomal/lysosomal system. *J. Cell Sci.* **113**, 2093-2101.

Ropolo, A., Grasso, D., Pardo, R., Sacchetti, M. L., Archange, C., Re, A. L., Seux, M., Nowak, J., Gonzalez, C. D., Iovanna, J. L. et al. (2007). The pancreatitis-induced vacuole membrane protein 1 triggers autophagy in mammalian cells. *J. Biol. Chem.* **282**, 37124-37133.

Saitoh, T., Nakayama, M., Nakano, H., Yagita, H., Yamamoto, N. and Yamaoka, S. (2003). TWEAK induces NF- B2 p100 processing and long lasting NF- $_{\kappa}$B activation. *J. Biol. Chem.* **278**, 36005-36012.

Saitoh, T., Fujita, N., Hayashi, T., Takahara, K., Satoh, T., Lee, H., Matsunaga, K., Kageyama, S., Omori, H., Noda, T. et al. (2009). Atg9a controls dsDNA-driven dynamic translocation of STING and the innate immune response. *Proc. Natl. Acad. Sci. USA* **106**, 20842-20846.

Shibutani, S. T. and Yoshimori, T. (2014). A current perspective of autophagosome biogenesis. *Cell Res.* **24**, 58-68.

Shirahama-Noda, K., Kira, S., Yoshimori, T. and Noda, T. (2013). TRAPPIII is responsible for vesicular transport from early endosomes to Golgi, facilitating Atg9 cycling in autophagy. *J. Cell Sci.* **126**, 4963-4973.

Takahashi, Y., Meyerkord, C. L., Hori, T., Runkle, K., Fox, T. E., Kester, M., Loughran, T. P. and Wang, H.-G. (2011). Bif-1 regulates Atg9 trafficking by mediating the fission of Golgi membranes during autophagy. *Autophagy* **7**, 61-73.

Tanida, I., Minematsu-Ikeguchi, N., Ueno, T. and Kominami, E. (2005). Lysosomal turnover, but not a cellular level, of endogenous LC3 is a marker for autophagy. *Autophagy* **1**, 84-91.

Webber, J. L. and Tooze, S. A. (2010). Coordinated regulation of autophagy by p38α MAPK through mAtg9 and p38IP. *EMBO J.* **29**, 27-40.

Young, A. R. J., Chan, E. Y. W., Hu, X. W., Kochl, R., Crawshaw, S. G., High, S., Hailey, D. W., Lippincott-Schwartz, J. and Tooze, S. A. (2006). Starvation and ULK1-dependent cycling of mammalian Atg9 between the TGN and endosomes. *J. Cell Sci.* **119**, 3888-3900.

Zavodszky, E., Seaman, M. N. J., Moreau, K., Jimenez-Sanchez, M., Breusegem, S. Y., Harbour, M. E. and Rubinsztein, D. C. (2014). Mutation in VPS35 associated with Parkinson's disease impairs WASH complex association and inhibits autophagy. *Nat. Commun.* **5**, 3828.

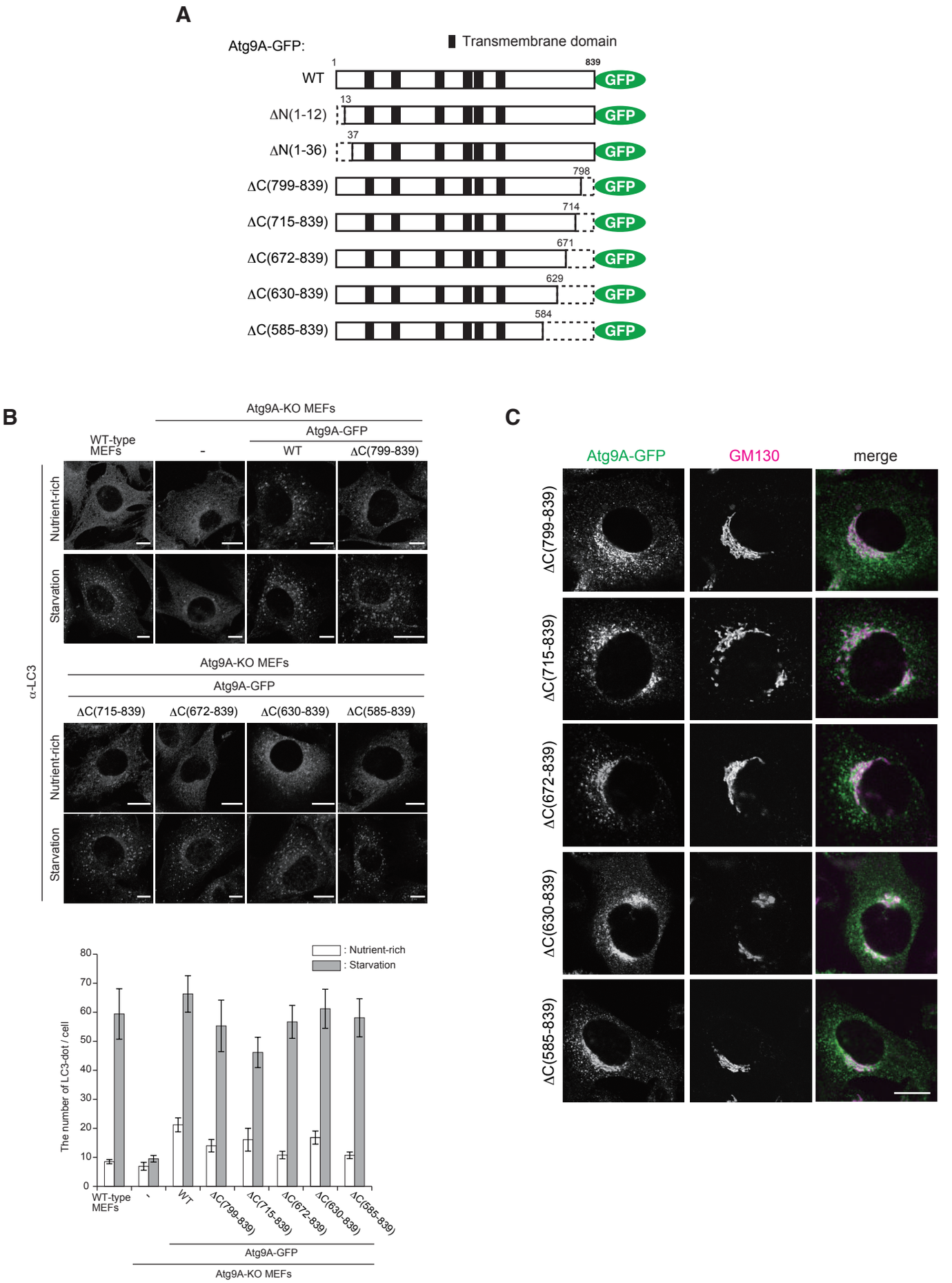

Figure S1. The C-terminal deletions of Atg9A dose not affect autophagosome formation and its localization.

(A) Schematic diagram of wild-type Atg9A and its deletion mutants tagged with GFP. The transmembrane domain is indicated as black boxes. (B) Wild-type or Atg9A-KO MEFs stably expressing the indicated constructs were cultured in growth medium (Nutrient-rich) or EBSS (Starvation) for 1 h, then analyzed by immunocytochemistry for LC3. The number of LC3 puncta in each cell was counted for more than 30 cells. The average ± SD is shown for three independent experiments. Bar, 20 µm. (C) Atg9A-KO MEFs stably expressing the indicated constructs were analyzed by immunocytochemistry for anti-GM130. Bar, 20 µm.

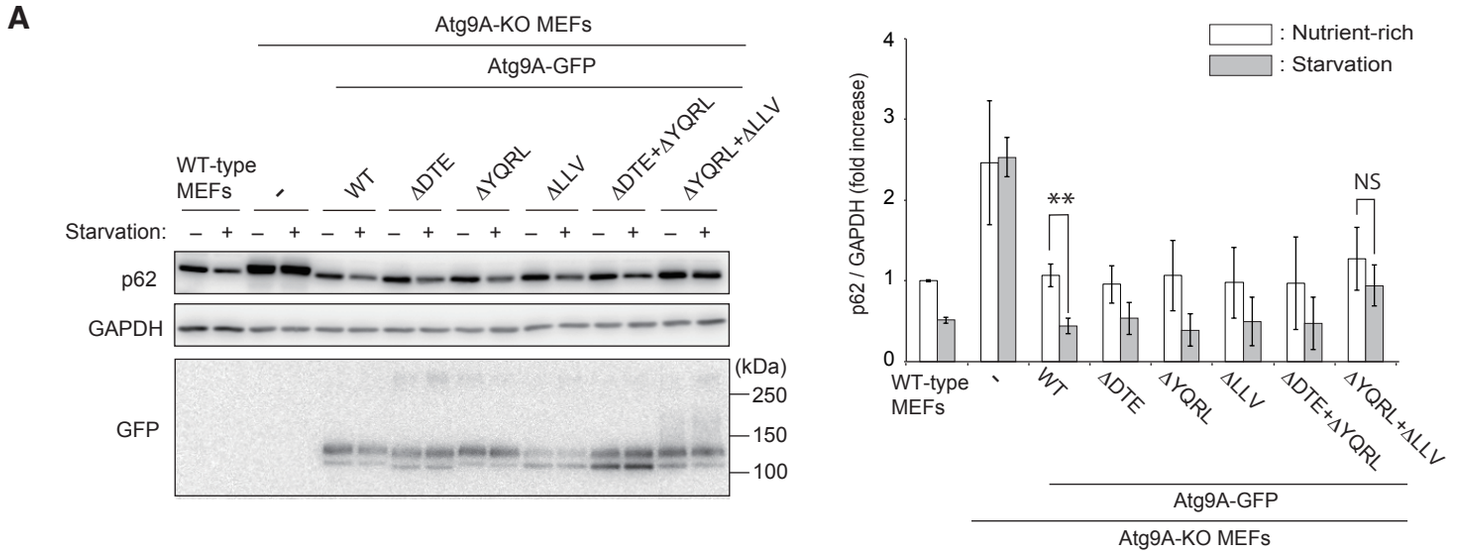

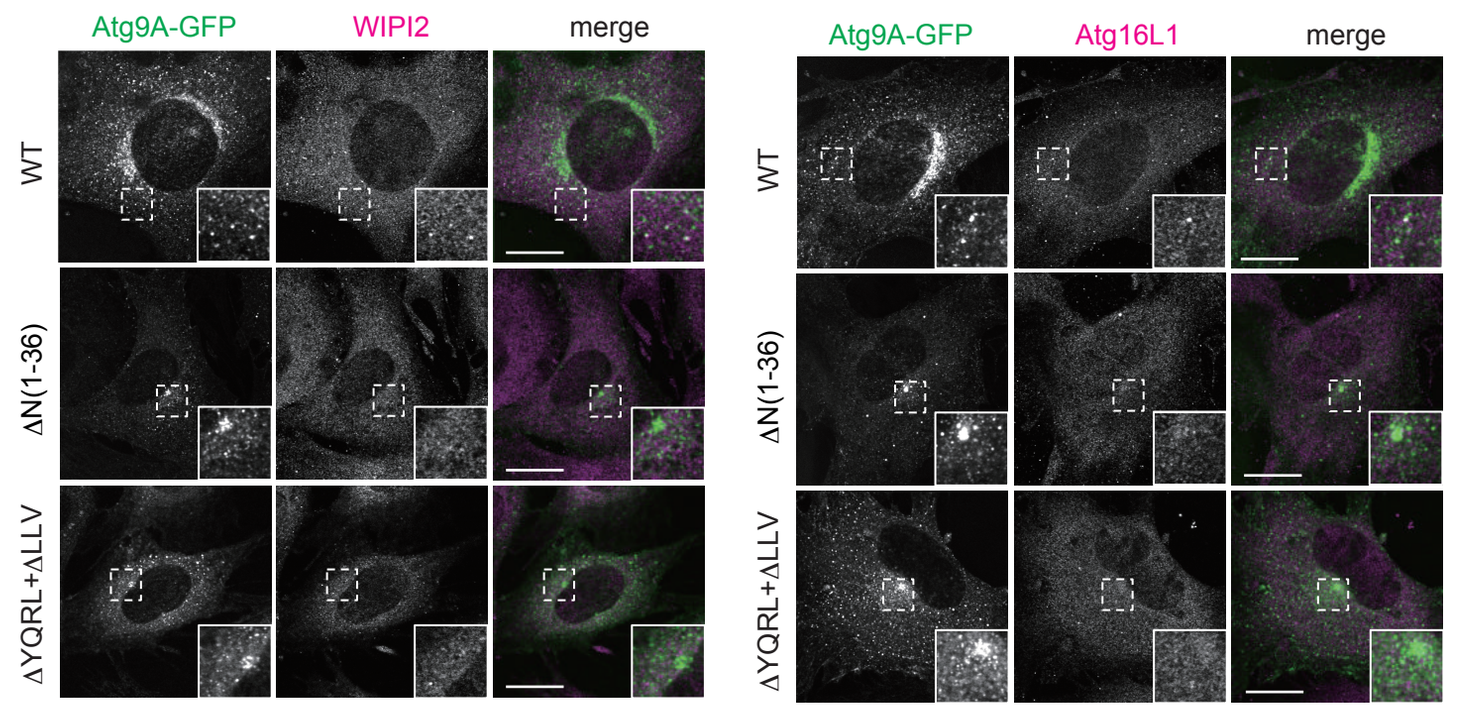

Figure S2. The effects of alanine substitutions in sorting motifs on autophagy.

(A) Wild-type MEFs or Atg9A-KO MEFs stably expressing the indicated constructs were cultured in growth medium (Nutrient-rich) or EBSS (Starvation) for 2 h, and subjected to western blotting using indicated antibodies. The graph indicates the p62 signal relative to GAPDH. The average ±SD is shown for three independent experiments. Statistical analysis was performed by two-tailed paired Student' s t-test: **, $P < 0.01$; NS, not significant. (B) Atg9A-KO MEFs stably expressing the indicated constructs were cultured in EBSS (Starvation) for 1 h, fixed, and then analyzed by immunocytochemistry for anti-WIPI2 or anti-Atg16L1. Bar, 20 μm.

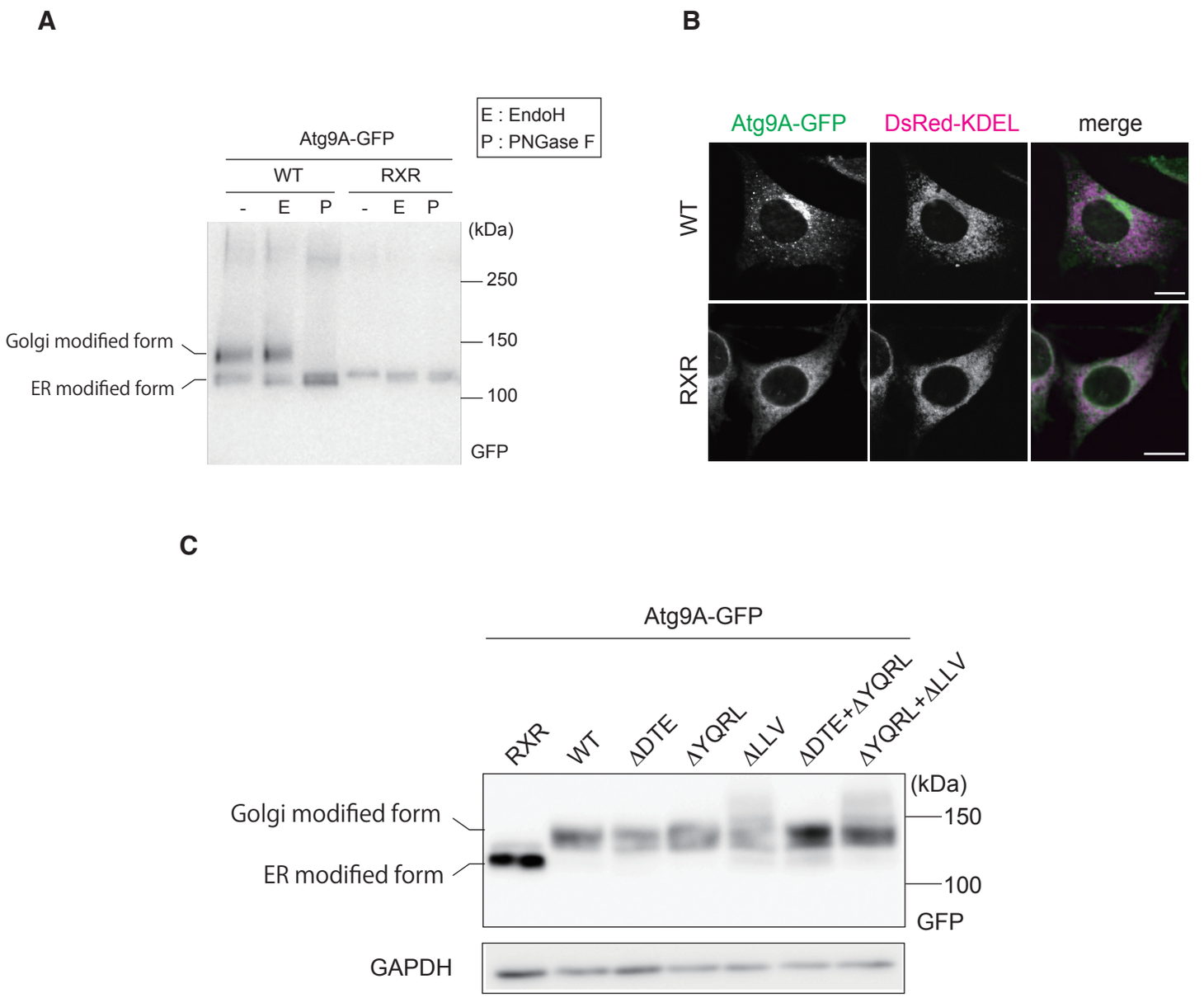

Figure S3. The effects of alanine substitutions in sorting motifs on N-glycan modification of Atg9A.

(A) Atg9A-KO MEFs stably expressing the indicated constructs were lysed and subjected to treatment with EndoH or PNGase F, and analyzed by western blotting with anti-GFP. Atg9A-WT-EGFP was detected as two major bands by western blotting. When the sample was treated with endoglycosidase H (Endo H) which removes only high mannose and some hybrid types of N-glycan from glycoproteins (Maley et al., 1989), the faster migrating band was shifted slightly, whereas the slower migrating band was resistant to EndoH. Treatment with N-Glycosidase F (PNGase F), which removes all N-glycan from glycolproteins (Maley et al., 1989), resulted in mobility shift of both bands to a single band. (B) Atg9A-KO MEFs stably expressing the indicated constructs were transiently transfected with pDsRed-KDEL expression plasmid, fixed, and examined by fluorescence microscopy. When RXR motif, the ER retrieval signal, was added to its C-terminus of Atg9A, the mutant showed good colocalization with an ER marker (DsRed-KDEL) (C) Atg9A-KO MEFs stably expressing the indicated constructs were lysed and analyzed by western blotting with anti-GFP.

Maley, F., Trimble, R. B., Tarentino, A. L. and Plummer, T. H. Jr. (1989). Characterization of glycoproteins and their associated oligosaccharides through the use of endoglycosidases. *Anal. Biochem.* **180**, 195-204.

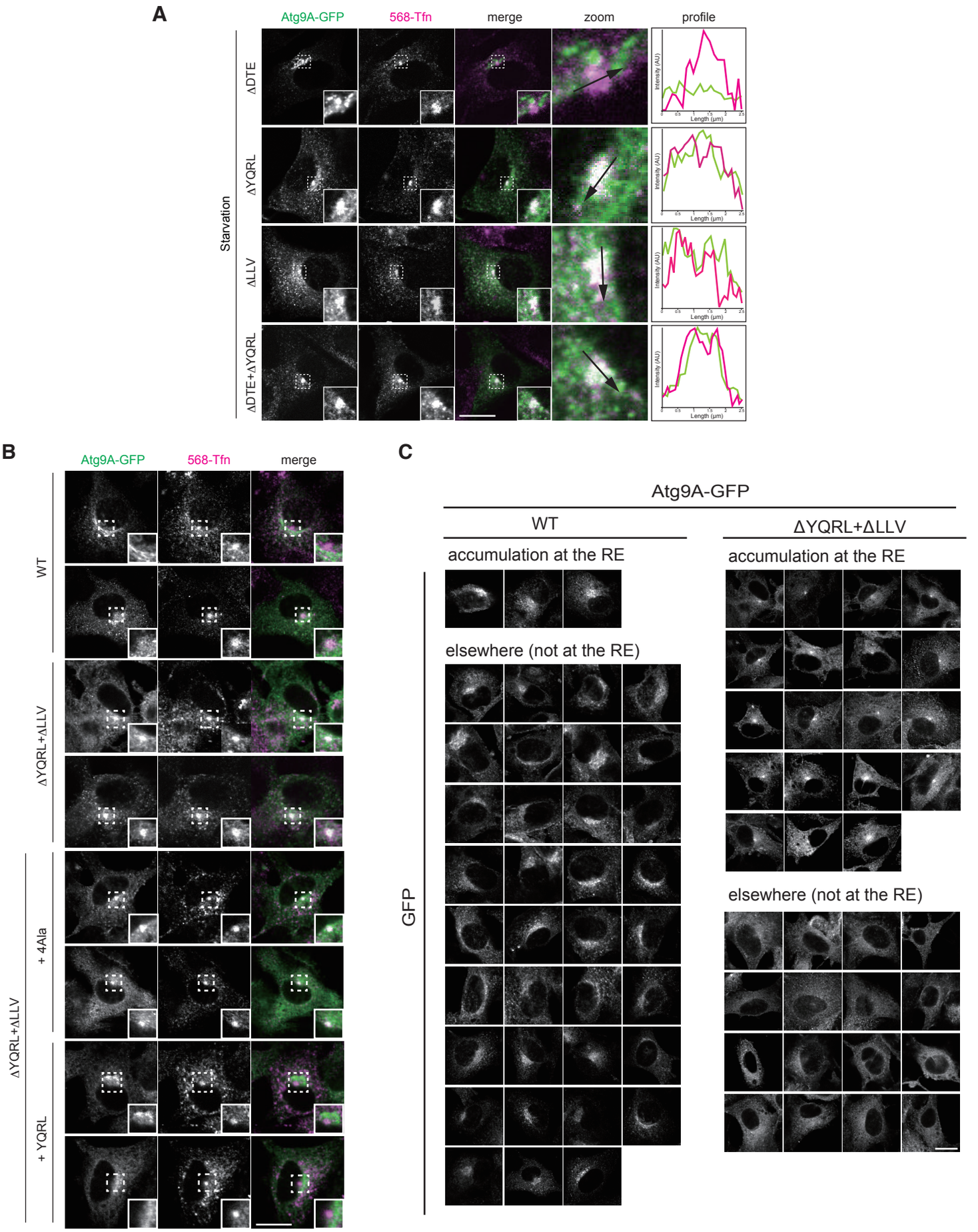

Figure S4. The effects of alanine substitutions in sorting motifs on Atg9A localization.

(A-B) Atg9A-KO MEFs stably expressing the indicated constructs were cultured in EBSS (Starvation) with 10 μg/ml 568-Tfn for 1 h, and then observed by fluorescence microscopy. Bar, 20 μm. (C) Atg9A-KO MEFs stably expressing indicated constructs were cultured in EBSS (Starvation) with 10 μg/ml 568-Tfn for 1 h, fixed, and then observed by fluorescence microscopy. Bar, 20 μm. Examples of Atg9A accumulated at the recycling endosomes (RE) and remained in elsewhere (not at the RE) were shown for both WT and ΔYQRL+ΔLLV mutant cells. Atg9A WT showed the accumulation at the RE phenotype in only 7.9 % cells (3 of 38 total cell counted), while ΔYQRL+ΔLLV mutant showed in 54.3% cells (19 of 35 total cell counted).